Using the Selective Functionalization of Metallic Single-Walled Carbon Nanotubes to Control Dielectrophoretic Mobility

Seunghyun Baik,[†] Monica Usrey,[†] Lolita Rotkina,[‡] and Michael Strano*[,†]

Department of Chemical and Biomolecular Engineering, and Beckman Institute, University of Illinois, Urbana, Illinois 61801

Received: May 5, 2004; In Final Form: July 8, 2004

The effect of sidewall functionalization on the dielectrophoretic mobility of single-walled carbon nanotubes is investigated using a 10-μm electrode gap and an alternating current electric field of 10 V and 10 Mhz. For nanotubes dispersed in aqueous solution using 1% sodium dodecyl sulfate, a high degree of alignment is observed for material deposited across the gap. Raman spectroscopy at 632.8- and 785-nm excitation indicates that both metallic and semiconducting nanotubes are deposited. An apparent increase in metallic modes in the 632.8-nm spectrum is shown to be related to sample morphology and the choice of control material for comparison, not separation or enrichment. Electrical transport measurements reveal both a gate-voltage dependence as well as current at zero gate voltage, which is consistent with a mixture of metallic and semiconducting pathways. Alternatively, fewer nanotubes deposit in the gap when the metallic nanotubes are selectively functionalized using 1-chlorobenzene diazonium. The results suggest that either the functionalization itself or an adsorbed reagent has reversed the sign of the Clausius−Mossotti factor for metallic nanotubes. This chemical method could be used as a means of selectively manipulating and depositing a heterogeneous mixture of nanotubes in solution into an array of uniform electronic type.

Introduction

Single-walled carbon nanotubes (SWNT) have received considerable attention, particularly for nanoscale electronic applications.[1−4] Two hurdles are widely recognized as impeding the development of these devices: separation according to electronic properties and manipulation into individually addressable arrays. Because all known synthetic techniques result in mixtures of metallic, semimetallic, and semiconducting electronic types,[5−7] the first step in addressing the former hurdle remains the separation of metallic from semiconducting SWNT.[2,8−9] The differences in electronic structure arise from the quantization of the electronic wave function as the nanotube is conceptually formed from a graphene sheet.[10] The chirality vector (n, m) determines the electronic types: When $|n - m| = 3q$, where q is an integer, the nanotube is metallic or semimetallic, while remaining species are semiconducting.

The latter hurdle is being addressed by combining solution-phase processing methods to separate[8] and sort carbon nanotubes by length,[11] with electrophoretic approaches to place carbon nanotubes in specific locations and orientations. A polarizable particle dispersed in solution is subject to a force under a nonuniform electric field, because of the Coulomb interaction with the electric dipole induced in the particle, giving rise to movement referred to as dielectrophoresis.[12−13] This technique has been used to move submicrometer colloidal particles as well as particles larger than a few micrometers.[14−15] The approach has also been used for both alignment of nanotubes across an electrode gap[16−18] and apparent, preferential deposition of metallic nanotubes for separation.[19−20] The degree of alignment depends on frequency, and SWNT density depends on the magnitude of the electric field.[16] Krupke et al.[19] reported the selective deposition of metallic and semimetallic nanotubes over semiconducting nanotubes using ac-dielectrophoresis because of a relative difference in dielectric constants with respect to the D_2O solvent. An apparent enrichment of metallic tubes to 80% was suggested according to Raman spectroscopy, with the incomplete separation attributed to aggregates containing at least one metallic nanotube.

In this paper, we examine this result in greater detail by combining spectroscopic and electron transport, as well as compare the dielectrophoretic mobility of functionalized and nonfunctionalized single-walled carbon nanotubes. Electrical transport measurements and Raman spectroscopy at 785- and 632.8-nm excitaiton are used to characterize the deposited material and the extent of any preferential depostion of metallic over semiconducting nanotubes. It is found that the apparent enrichment of metallic nanotubes may be complicated by the choice of control for comparison and, particularly, its morphology. Functionalization of metallic nanotubes should disrupt the 1-D electronic structure and render them near insulating. Diazonium salts[8] have been shown to perform this chemistry. We seek to develop these chemical methods as means of selectively manipulating and depositing a heterogeneous mixture of nanotubes in solution into an array of uniform electronic types.

Experimental Section

Electrodes were fabricated by photolithography with a gap size of 10 μm and a length of 800 μm as shown in Figure 1. The contacts were formed on a SiO_2−Si substrate by sputtering 10 nm of titanium and 190 nm of gold. A drop of HiPco-SWNT

* To whom correspondence should be addressed. Mailing address: 118 Roger Adams Laboratory, Box C-3, 600 South Mathews Avenue, Urbana, IL 61801. E-mail: strano@uiuc.edu. Phone: (217)-333-3634. Fax: (217)-333-5052.

[†] Department of Chemical and Biomolecular Engineering.

[‡] Beckman Institute.

10.1021/jp048066u CCC: $27.50
Published on Web 09/10/2004

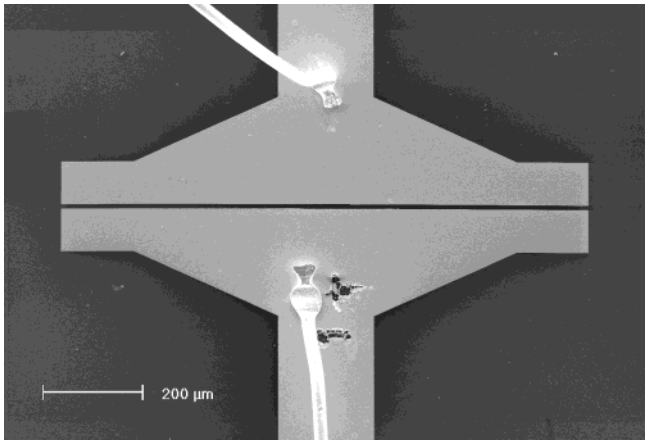

Figure 1. Electrode configuration used in this work.

(10 μL) dispersed using sodium dodecyl sulfate (SDS) surfactant (1% in D_2O by weight), prepared according to a previously published protocol,[21] was placed on the electrode after turning on the function generator at a frequency of 10 MHz and a peak-to-peak voltage of 10 V. The conditions are almost identical to those in ref 19. The function generator was turned off after the drop was blown away using nitrogen gas after a delay of 10 min. Electrical transport measurements were carried out using a semiconductor parameter analyzer (HP 4155A). A Raman microscope (Renishaw, inVia Reflex) was used at two excitation wavelengths. A HeNe laser with a grating of 1800 grooves/mm was used for 632.8-nm excitation, and a diode laser with a grating of 1200 grooves/mm was used for 785-nm excitation. The power of the laser was 17 mW for the former and 250 mW for the latter. The spot size was ~1−2 μm in diameter. Polarization of incident light was chosen perpendicular to the electrode gap.

Results and Discussion

Figure 2a shows a 10-μm gap at the center of the electrodes after dielectrophoresis. After application of the field for 10 min (10 V peak-to-peak, 10 MHz), carbon nanotubes dispersed using 1% SDS produce a mat of material which is aligned along the electric field. Nanotubes bridged the entire gap of the electrodes. Tens of picograms are estimated to deposit within the 10 × 800 μm^2 gap. The inset to Figure 2a provides the starting absorption spectrum of the solution, showing both metallic and semiconducting optical transitions. The spectrum monitors the valence (v) to conduction (c) electronic transitions indicating v1 → c1 transitions of metallic nanotubes from roughly 440 to 645 nm for HiPco nanotubes. The v1 → c1 and v2 → c2 transitions of the semiconducting nanotubes are in the ranges 830−1600 and 600−800 nm, respectively. Electrical transport measurements on the deposited material show both conduction at zero applied gate voltage and a modulation of the $I-V$ curve with changing gate voltage (Figure 2b). These observations are consistent with a mixture of metallic and semiconducting pathways, respectively.

In using micro-Raman spectroscopy to characterize the material in the gap, we compare with two different types of unseparated control samples. Both are produced from exactly the same starting solution as the dielectrophoretically deposited material. We have recently found that sample morphology (i.e., nanotube bundle size) can affect the relative intensities of Raman modes.[22] One control is prepared in a manner similar to the method used by Krupke et al.[19] and involves drying the solution on a substrate. The process creates large ropes approximately

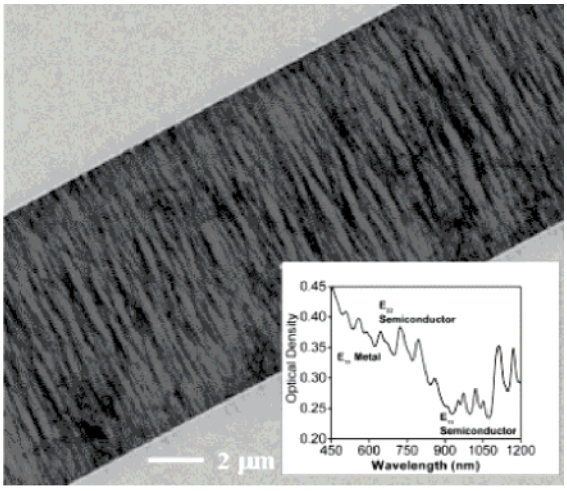

(a)

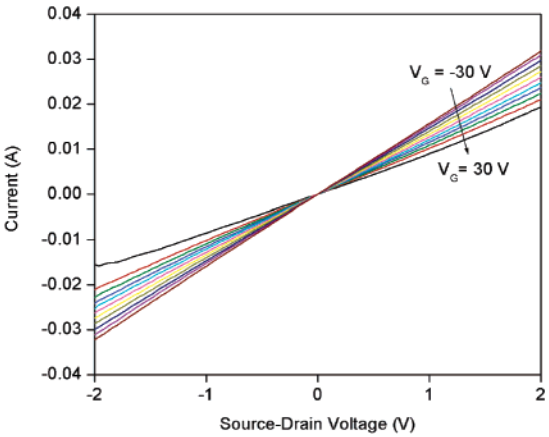

(b)

Figure 2. Electrode gap after deposition of nonfunctionalized SWNT using ac-dielectrophoresis. (a) SEM image. The absorption spectrum of the starting solution is shown in the lower right corner. (b) Source-drain current as a function of source-drain voltage. Gate voltage was changed from −30 to 30 V in steps of 6 V.

100 nm in thickness. Conversely, precipitating nanotubes from solution using acetone and subsequent washing creates smaller, 5−20-nm ropes. A detailed characterization and the associated changes in the Raman spectra is presented elsewhere.[22]

At 632.8-nm excitation, both metallic and semiconducting carbon nanotubes are in resonance for the HiPco material used in this work. Chiral vectors for metallic nanotubes are shown in bold italics. Compared to the large aggregate control (Figure 3a), there is an apparent, preferential enhancement of metallic modes for material dielectrophoretically deposited within the gap (Figure 3b). The area ratio of metallic over semiconducting modes increased about 40%. However, this enhancement is mimicked in the spectrum for smaller ropes (Figure 3c). The similarities are also observed at 785-nm excitation (Figure 3d−f), which probes semiconducting nanotubes, exclusively. Spectral similarities between the smaller aggregate control and the material in the electrode gap suggest that the dielectrophoretic deposition under these conditions creates material with a similar morphology. Consequently, there is no evidence of metallic enrichment under the conditions explored in this work, and the Raman spectra support the $I-V$ measurements in Figure 2b.

A dielectric particle experiences a force toward or away from the high field gradient near the electrode gap depending upon the sign of the real part of the Clausius−Mossotti factor (CM)

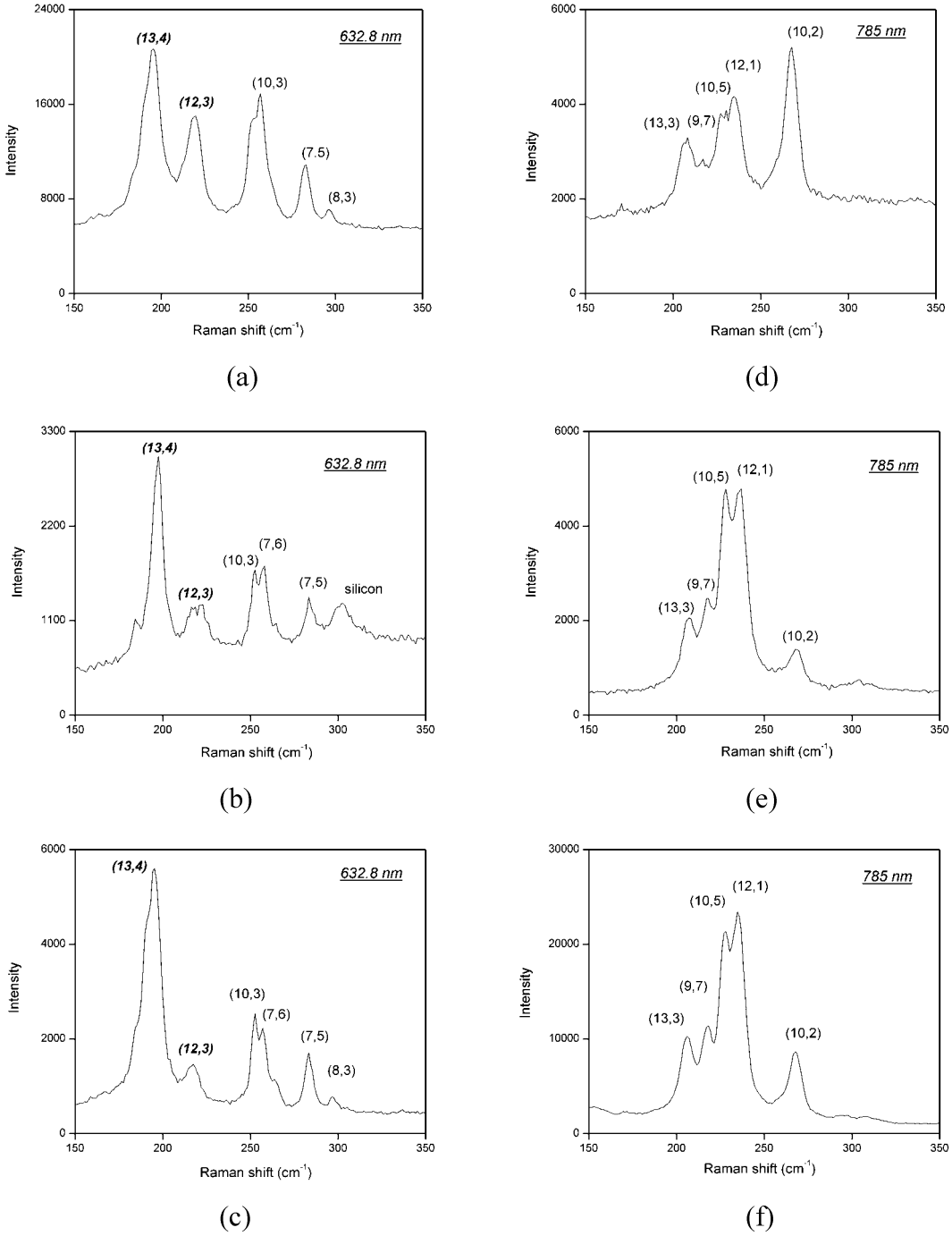

Figure 3. Raman spectra of the radial breathing mode regions of nonfunctionalized nanotubes. (a) Material dried on a glass slide at 632.8-nm excitation. (b) Dielectrophoretically deposited material at 632.8-nm excitation. (c) Acetone-flocked (see text) at 632.8-nm excitation. (d) Material dried on a glass slide at 785-nm excitation. (e) Dielectrophoretically deposited material at 785-nm excitation. (f) Acetone-flocked (see text) at 785-nm excitation.

for an assumed spherical dielectric particle in a dielectric medium.[12,23]

$$f_{CM} = \frac{\overline{\epsilon_p} - \overline{\epsilon_m}}{\overline{\epsilon_p} + 2\overline{\epsilon_m}} \quad (1)$$

Although eq 1 is correct only for spherical particles, it nevertheless shows frequency dependence based on the complex permittivity of the particle, $\overline{\epsilon_p}$, and the surrounding medium, $\overline{\epsilon_m}$. Previous researchers[19] argue that the static dielectric constant of semiconducting carbon nanotubes, which is inversely proportional to the square of the band gap energy,[24] is less than 5, while the value of metallic nanotubes should be exceedingly high or infinite. From this, negative and positive values of the CM factor are calculated that predict a separation between the two types as metals are preferentially deposited.[19] However, this argument neglects the frequency dependence of the complex permittivity that involves both the medium, κ_m, and particle, κ_p, conductivity:

$$\overline{\epsilon_p} = \epsilon_p - i\left(\frac{\kappa_p}{\omega}\right) \quad (2)$$

$$\overline{\epsilon_m} = \epsilon_m - i\left(\frac{\kappa_m}{\omega}\right) \quad (3)$$

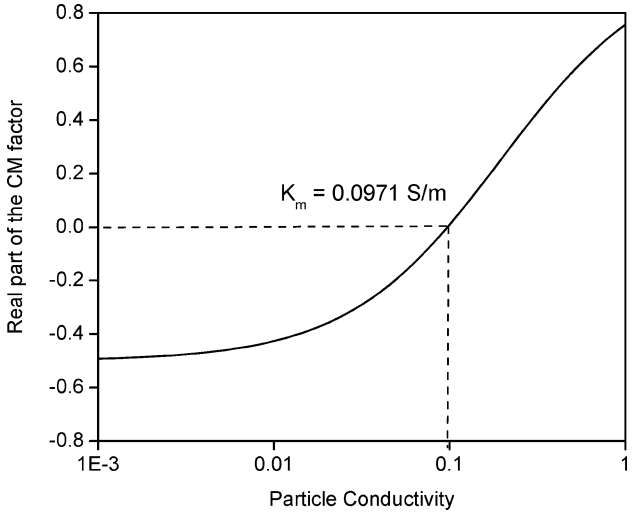

Figure 4. Real part of the Clausius−Mossotti factor as a function of κ_p for semiconducting carbon nanotubes assuming values of $\epsilon_p = 5$ and $\epsilon_m = 80$. The conductivity of a 1% SDS/D_2O solution ($\kappa_m = 0.0971$ S/m) was measured.

Figure 4 plots the predicted CM factor as a function of κ_p for semiconducting carbon nanotubes, assuming values of $\epsilon_p = 5$ and $\epsilon_m = 80$. A conductivity cell (Thermo Electron Corporation, Orions 013005A) with a nominal cell constant of 0.475 cm^{-1} was used to measure the conductivity of a 1% SDS/D_2O solution (κ_m) as 0.0971 S/m. If the assumption of infinite ϵ_p for metallic nanotubes is valid, positive dielectrophoresis will always be observed, and these nanotubes will deposit into the gap. However, negative or positive dielectrophoresis is predicted for semiconducting nanotubes (or even insulating particles) depending upon the conductivity of the medium, κ_m, and that of the particle, κ_p. Figure 4 shows that at 10 MHz a semiconducting nanotube with an assumed $\epsilon_p = 5$ displays either positive (toward the electrode) or negative (repulsion) dielectrophoresis depending on whether the particle conductivity is greater or less than that of the medium, respectively. This apparent particle conductivity in an electrolyte is, in turn, the sum of three identified contributions:[12]

$$\kappa_m = \kappa_{int} + \kappa_{sur} + \kappa_\alpha \quad (4)$$

The intrinsic particle value, κ_{int}, can be augmented by conductivity due to adsorbed ions that migrate to transport charge, κ_{sur}, even on an insulating particle. The last term, from the so-called α-dispersion, is believed to arise from the charged double layer around the particle, κ_α. The second and third terms are surface conduction contributions which depend on particle size, and these effects can augment the conductivity by many times the intrinsic value.[12] The model predicts that metal/semiconductor separation may be possible by increasing the medium conductivity at a constant nanotube surface charge and may provide an explanation for why both metallic and semiconducting species are observed under the conditions of this work.

Dielectrophoretic behavior is significantly altered upon selective functionalization of metallic nanotubes. Figure 5a shows dielectrophoretically deposited material, at the center of the electrodes, from a sample where metallic nanotubes were selectively functionalized using diazonium salts, as reported previously.[8] On the average, substantially fewer nanotubes deposited in the gap, and the alignment is poor compared to Figure 2a. The absorption spectrum of the starting material is shown in the inset to Figure 5a and indicates selective attenuation of metallic optical transitions. This has been interpreted as a

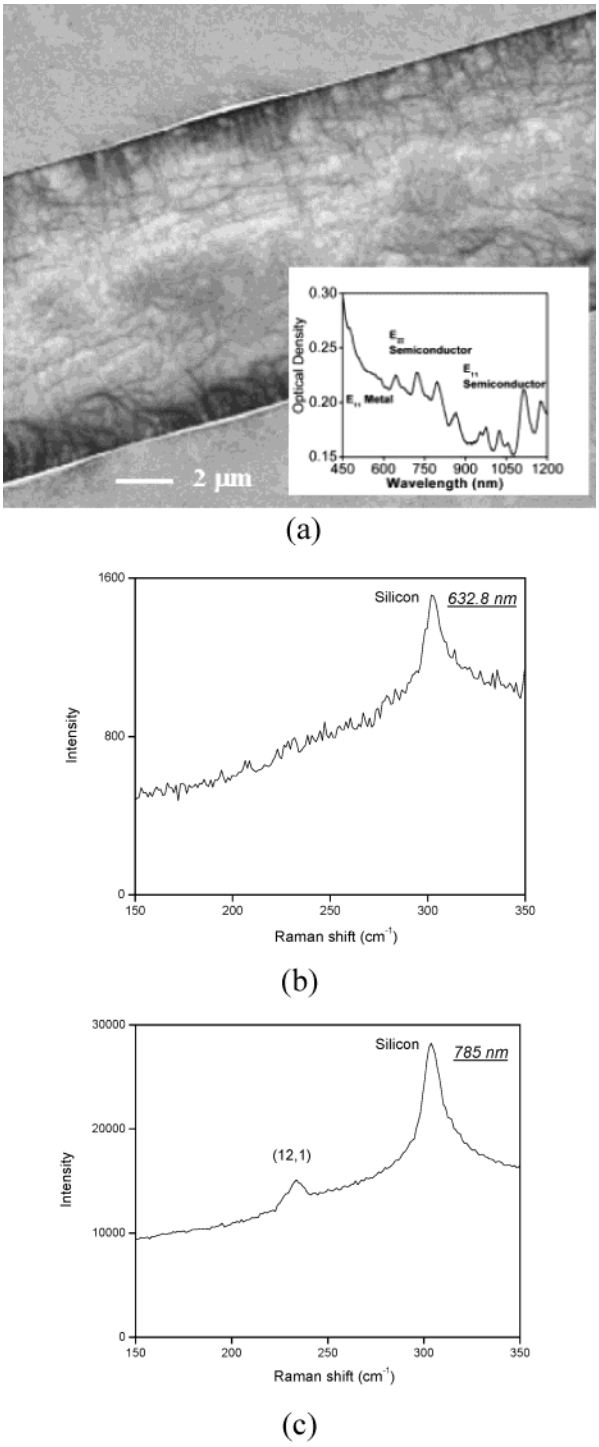

Figure 5. Electrode gap after deposition of selectively functionalized SWNT using ac-dielectrophoresis. (a) SEM image. The absorption spectrum of the starting solution is shown in the lower right corner. (b) Raman spectra of the radial breathing mode regions at 632.8-nm excitation. (c) Raman spectra of the radial breathing mode regions at 785-nm excitation.

sidewall addition to the metallic nanotubes and is anticipated to lower the intrinsic conductivity of these species. We see no Raman modes from material in the gap at 632.8-nm excitation (Figure 5b), while the (12, 1) species is visible at 785 nm (Figure 5c). We attribute these to the differences in maximum laser power available for each wavelength; therefore, Raman features are lower than the detection limit in the case of 632.8 nm.

The results suggest that the functionalization itself or the presence of excess reagent has reversed the sign of the CM

factor for a sizable fraction of nanotubes in the sample. The added salt (0.1 mM) is too low in concentration to appreciably affect κ_m. For metallic nanotubes, the expected decrease in intrinsic conductivity and dielectric constant predicts a reversal of the CM factor, and the absence of deposited material is consistent. Balasubramanian and co-workers[25] observe a 10^6 reduction in conduction through metallic pathways upon functionalization using diazonium salts. However, our model dictates that the functionalization also disrupt surface conduction caused by ions in order to reverse the dielectrophoresis ($\kappa_{sur} \approx 0$). It is plausible that sidewall functionalization sterically impedes ion mobility on the surface. Semiconductors, whose optical transitions are not significantly affected by the functionalization process, should still deposit into the gap. This is consistent with the spectroscopic evidence in Figure 5b−c, although the quantity is disproportionately reduced, and alignment is not as prominent. A more detailed investigation of the causes of this is currently underway.[26]

Conclusion

In summary, the relative intensities of metallic modes increase for the nonfunctionalized nanotubes deposited dielectrophoretically. However, we attribute the increases to changes in morphology between the control and deposited material. The effect of sidewall functionalization on the dielectrophoretic mobility of single-walled carbon nanotubes is analyzed. Both nonfunctionalized and selectively functionalized nanotubes are deposited on a microelectrode gap, and the characteristics of the resulting material are examined by current−voltage measurements and Raman spectroscopy. A relatively higher density of nanotubes is deposited with a high degree of alignment for the case of nonfunctionalized nanotubes. However, only smaller concentrations of nanotubes are deposited for the selectively funcionalized nanotubes, suggesting that diazonium reagents greatly affect the dielectric function of metallic nanotubes.

Acknowledgment. This work was supported by the School of Chemical Sciences at the University of Illinois at Urbana-Champaign and a grant from the National Science Foundation (CTS-0330350). A. Gaur and J. Rogers are acknowledged for their assistance with semiconductor parameter measurements. T. Prusnick and R. Bormett at Renishaw are acknowledged for assistance with micro-Raman measurements.

References and Notes

(1) McEuen, P. *Phys. World* **2000**, *13*, 31.
(2) Avouris, P. *Acc. Chem. Res.* **2002**, *35*, 1026.
(3) Yao, Z.; Kane, C. L.; Dekker, C. *Phys. Rev. Lett.* **2000**, *84*, 2941.
(4) Tans, S. J.; Verschueren, A. R. M.; Dekker, C. *Nature* **1998**, *393*, 49.
(5) Bronikowski, M. J.; Willis, P. A.; Colbert. D. T.; Smith, K. A.; Smalley, R. *J. Vac. Sci. Technol.* **2001**, *19*, 1800.
(6) Saito, R.; Dresselhaus, G.; Dresselhaus, M. S. *Physical Properties of Carbon Nanotubes*; Imperial College Press: London, 1998
(7) Thess, A.; Lee, R.; Nikolaev, P.; Dai, H. J.; Petit, P.; Robert, J.; Xu, C. H.; Lee, Y. H.; Kim, S. G.; Rinzler, A. G.; Colbert, D. T.; Scuseria, G. E.; Tomanek, D.; Fischer, J. E.; Smalley, R. E. *Science* **1996**, *273*, 483.
(8) Strano, M. S.; Dyke, C. A.; Usrey, M. L.; Barone, P. W.; Allen, M. J.; Shan, H.; Kittrell, C.; Hauge R. H.; Tour, J. M.; Smalley, R. E. *Science* **2003**, *301*, 1519.
(9) Krupke, R.; Hennrich, F.; Weber, H. B.; Kappes, M. M.; Lohneysen, H. V. *Nano Lett.* **2003**, *3*, 1019.
(10) Dresselhaus, M. S.; Dresselhaus, G.; Eklund, P. C. *Science of fullerenes and carbon nanotubes*; Academic Press: San Diego, CA, 1996.
(11) Heller, D. A.; Mayrhofer, R. M.; Baik, S.; Grinkova, Y. V.; Usrey, M. L.; Strano, M. S. *J. Am. Chem. Soc.*, submitted for publication, 2004.
(12) Green, N. G.; Morgan, H. *J. Phys. Chem. B* **1999**, *103*, 41.
(13) Pohl, H. A. *Dielectrophoresis*; Cambridge University Press: New York, 1978
(14) Green, N. G.; Milner, J. J.; Morgan, H. *J. Biochem. Biophys. Methods* **1997**, *35*, 89.
(15) Hughes, M. P.; Morgan, H.; Rixon, F.; Burt, J. P. H.; Pethig, R. *Biochim. Biophys. Acta* **1998**, *1425*, 119.
(16) Chen, X. Q.; Saito, T.; Yamada, H.; Matsushige, K. *Appl. Phys. Lett.* **2001**, *78*, 3714.
(17) Nagahara, L.; Amlani, I.; Lewenstein, J.; Tsui, R. *Appl. Phys. Lett.* **2002**, *80*, 3826.
(18) Krupke, R. *Appl. Phys. A* **2003**, *76*, 397.
(19) Krupke, R.; Hennrich, F.; Lohneysen, H. V.; Kappes, M. M. *Science* **2003**, *301*, 344.
(20) Lee, S. W.; Lee, D. S.; Yu, H. Y.; Campbell, E. E. B.; Park, Y. W. *Appl. Phys. A* **2004**, *78*, 283.
(21) O'Connell, M. J.; Bachilo, S. M.; Huffman, C. B.; Moore, V. C.; Strano, M. S.; Haroz, E. H.; Rialon, K. L.; Boul, B. J.; Noon, W. H.; Kitrell, C.; Ma, J.; Hauge, R. H.; Weisman, R. B.; Smalley, R. E. *Science* **2002**, *297*, 593.
(22) Heller, D. A.; Barone, P. W.; Swanson, J. P.; Mayrhofer, R. M.; Strano, M. S. *J. Phys. Chem. B* **2004**, *108*, 6905.
(23) Jones, T. B. *Electromechanisms of Particles*; Cambridge University Press: Cambridge, 1995
(24) Benedict, L. X.; Louie, S. G.; Cohen, M. L. *Phys. Rev. B* **1995**, *52*, 8541.
(25) Balasubramanian, K.; Sordan, R.; Burghard, M.; Kern, K. *Nano Lett.* **2004**, *4*, 827.
(26) Rotkina, L.; Baik, S.; Strano, M. S. Manuscript in preparation.